

Cumulative reaction probabilities and transition state properties: A study of the $F + H_2$ reaction and its deuterated isotopic variants

Cite as: J. Chem. Phys. **129**, 024305 (2008); <https://doi.org/10.1063/1.2952672>

Submitted: 10 March 2008 . Accepted: 06 June 2008 . Published Online: 14 July 2008

F. J. Aoiz, V. J. Herrero, and V. Sáez Rábanos



View Online



Export Citation

ARTICLES YOU MAY BE INTERESTED IN

Cumulative reaction probabilities: A comparison between quasiclassical and quantum mechanical results

The Journal of Chemical Physics **125**, 144105 (2006); <https://doi.org/10.1063/1.2353837>

An experimental study of $OH(A^2\Sigma^+) + H_2$: Electronic quenching, rotational energy transfer, and collisional depolarization

The Journal of Chemical Physics **146**, 244313 (2017); <https://doi.org/10.1063/1.4989567>

Rate coefficients from quantum and quasi-classical cumulative reaction probabilities for the $S(^1D) + H_2$ reaction

The Journal of Chemical Physics **137**, 164314 (2012); <https://doi.org/10.1063/1.4761894>

Lock-in Amplifiers
up to 600 MHz



Cumulative reaction probabilities and transition state properties: A study of the $F+H_2$ reaction and its deuterated isotopic variants

F. J. Aoiz,^{1,a)} V. J. Herrero,^{2,b)} and V. Sáez Rábanos^{3,c)}

¹*Departamento de Química Física, Facultad de Química, Universidad Complutense, 28040 Madrid, Spain*

²*Instituto de Estructura de la Materia (CSIC), Serrano 123, 28006 Madrid, Spain*

³*Departamento de Química y Bioquímica, ETS Ingenieros de Montes, Universidad Politécnica, 28040 Madrid, Spain*

(Received 10 March 2008; accepted 6 June 2008; published online 14 July 2008)

A comparative quantum mechanical (QM) and quasiclassical trajectory (QCT) study of the cumulative reaction probabilities (CRPs) is presented in this work for the $F+H_2$ reaction and its isotopic variants for low values of the total angular momentum J . The agreement between the two sets of calculations is very good with the exception of some features whose origin is genuinely QM. The agreement also extends to the CRP resolved in the helicity quantum number k . The most remarkable feature is the steplike structure, which becomes clearly distinct when the CRPs are resolved in odd and even rotational states j . The analysis of these steps shows that each successive increment is due to the opening of the consecutive rovibrational states of the H_2 or D_2 molecule, which, in this case, nearly coincide with those of the transition state. Moreover, the height of each step reflects the number of helicity states compatible with a given J and j values, thus indicating that the various helicity states for a specific j have basically the same contribution to the CRPs at a given total energy. As a consequence, the dependence with k of the reactivity is practically negligible, suggesting very small steric restrictions for any possible orientation of the reactants. This behavior is in marked contrast to that found in the $D+H_2$ reaction, wherein a strong k dependence was found in the threshold and magnitude of the CRP. The advantages of a combined QCT and QM approaches to the study of CRPs are emphasized in this work. © 2008 American Institute of Physics.
[DOI: 10.1063/1.2952672]

I. INTRODUCTION

The $F+H_2$ reaction remains to this day the main prototype of an exothermic elementary chemical reaction. This reactive system has received a great deal of attention over the last four decades. Since the 1960s, chemical laser¹ and chemiluminescence² experiments have showed that the product molecules were formed with a strong population inversion. In the 1980s, the landmark experiments of Lee and co-workers^{3,4} provided the vibrationally state-resolved differential cross sections (DCSS) for $F+H_2$ and its deuterated isotopic variants. Further molecular beam⁵⁻⁷ and photodetachment⁸⁻¹⁰ experiments added to the details during the 1990s. The experiments of Lee and co-workers revealed characteristic forward-scattering peaks in some of the products of vibrational states that were tentatively attributed to scattering resonances, but the theoretical interpretation of these results proved to be challenging due mostly to the lack of a precise potential energy surface (PES). By the mid-1990s, an accurate PES was finally released by Stark and Werner (hereafter SW-PES).¹¹ Quantum mechanical (QM) and quasiclassical trajectory (QCT) calculations of integral and DCS and rate constants on the SW-PES could reproduce the available experimental data with comparatively small

discrepancies,¹²⁻¹⁹ and the resonance interpretation of the forward peaks observed in the experiments of Lee and co-workers was questioned.^{12,17} Later works combining molecular beams and laser techniques with precise QM calculations explored the contribution of the two spin-orbit states of F to the reactivity and provided clearer evidence for the presence of scattering resonances at low collision energies.²⁰⁻³³

Although scattering resonances are very sensitive to peculiarities of the PES in the vicinity of the transition state (TS), they usually make a small contribution to the total rate coefficient. A convenient connection between TS properties and rate coefficients can be established through the cumulative reaction probability (CRP). This quantity was introduced by Miller in the 1970s,³⁴⁻³⁸ and since then, it has received a great deal of attention in the literature. Its usage provides a powerful link between the dynamics of a reaction and the structure of its TS and has allowed the precise determination of quantum effects such as Feshbach or shape-type resonances. The CRP is a measure of the effective number of reagent states that can lead to the formation of products at a given energy. In general, the CRP grows with energy in a way that depends on the shape of the PES at the TS and shows a more or less smooth step structure related, in principle, with the quantized levels of the activated complex, which are often termed as quantum bottleneck states (QBSs).³⁹⁻⁵⁰

In recent works, Aoiz *et al.* presented a methodology for the QCT calculation of CRPs.^{51,52} The method was validated

^{a)}Electronic mail: aoiz@quim.ucm.es.

^{b)}Electronic mail: vherrero@iem.cfmac.csic.es.

^{c)}Electronic mail: v.saez@upm.es.

through a successful comparison to accurate QM results for the $\text{H}+\text{H}_2$ and $\text{D}+\text{H}_2$ reactions. One of the most salient results was the presence of a smooth step structure in the QCT CRPs in a fairly good agreement with that obtained in QM results. Moreover, a series of maxima and minima was also found in the QCT density of reactive states (the derivative of the CRP with respect to the total energy) that resemble, sometimes very closely, those obtained in QM calculations, which have been attributed to the signatures of the TS.^{42,43} Since no quantization of the TS was contemplated in the QCT calculations, the origin of these structures in the QCT case had to be related to the quantization of the reactant states used in the QCT method. However, trajectories starting at a given, well-defined initial internal state tend to preserve this state in a statistical quasiadiabatic way from the reactant's asymptote to the TS,⁵³ and that would explain the observed behavior. In addition, in a combined QCT and QM study of the $\text{D}+\text{H}_2$ reaction, the threshold of the CRP was observed to increase with growing helicity quantum number k of the H_2 molecule.⁵² The good accordance between the QM and QCT results indicates that the threshold shift with k , attributed to QBS restrictions,^{47–50} can also be explained as a result of steric constraints imposed by the PES.⁵² This stereodynamical explanation is consistent with the interpretation based on the QBS, but in a way is more general since it does not require the explicit quantization of the TS.

In the present work, the CRP methodology that is commented on in the previous paragraph has been applied to the investigation of the $\text{F}+\text{H}_2$ reaction and isotopic variants whose TS properties differ markedly from those of $\text{H}+\text{H}_2$. Whereas the $\text{H}+\text{H}_2$ system has a high energy barrier with a steep bending potential favoring a collinear arrangement at the TS, the PES of $\text{F}+\text{H}_2$ is characterized by a low barrier with a flat bending potential and a bent TS.^{11,54–56} The reflection of these different TS on the CRPs for these two reactions was addressed by Chatfield *et al.*⁴³ Steric hindrances are appreciably smaller in the latter reaction. In addition, the early nature of the TS corresponds to a relatively separated F atom with respect to the H_2 molecule, which, to a large extent, conserves its own entity. In the course of this study, special emphasis has been laid on the dependence of the reactivity on reagent helicity on the variations of the CRP for the various isotopic variants and on the comparison between QM and classical data.

II. METHOD

This section reviews the main expressions used for the calculation of QM and QCT CRPs. Further details about the calculation procedures can be found in Refs. 51, 52, and 57.

A. Quantum CRPs

The reaction probability at a fixed total angular momentum, summed over product states but resolved with regard to reagent states, is related to the elements of the helicity representation scattering matrix (S) by

$$P_{vjk}^J(E) = \sum_{v',j',k'} |S_{v'j'k',vjk}^J|^2, \quad (1)$$

where the summation runs over all product states that are accessible at a given total energy. Note that a single arrangement for the products is implicitly assumed; if the number of possible product arrangements is larger, the summation of Eq. (1) must also run over all product arrangements. For simplicity, we have dropped the arrangement index from the notation.

CRPs are obtained by the summation of the reaction probability in Eq. (1) over reagent states. The summation over all reagent quantum numbers leads to the standard CRP,

$$C_r^J(E) = \sum_{v,j,k} P_{vjk}^J(E), \quad (2)$$

whereas the summation over vibrational and rotational quantum numbers only leads to the helicity-dependent CRP,

$$C_r^{J,k}(E) = \sum_{v,j} P_{vjk}^J(E). \quad (3)$$

All dynamical calculations were performed on the Stark-Werner (SW) PES.¹¹ For the quantum scattering calculations, we have used the coupled-channel hyperspherical coordinate method of Skouteris *et al.*⁵⁸

Converged CRPs were obtained for $J=0-2$ at total energies up to 0.8 eV and with a basis set including all $\text{F}+\text{H}_2$, HD, and D_2 channels with diatomic energies up to $E_{\text{max}}=1.8$ eV.

B. Quasiclassical CRPs

The QCT method to determine CRPs has been described in detail in previous publications.^{51,52} The initial conditions for each trajectory are sampled by quantizing the squares of the total \mathbf{J}^2 and the rotational \mathbf{j}^2 angular momenta, which are equated to $J(J+1)\hbar^2$ and $j(j+1)\hbar^2$, respectively. For each combination of (J, j) quantum (integer) numbers, the helicity quantum number k is chosen by uniform sampling with integer values in the $-\min(J, j) \leq k \leq \min(J, j)$ interval. With this sampling, the reaction probability at a given total energy and fixed total angular momentum, summed over product states but resolved with regard to reagent state, can be calculated as the ratio between the number of reactive trajectories (N_r) and the total number of trajectories (N) run under the given set of initial conditions (specified by the values of E, J, v, j , and k). One has

$$P_{vjk}^J(E) = \frac{N_r(E, J; v, j, k)}{N(E, J; v, j, k)}, \quad (4)$$

which is the quasiclassical counterpart of Eq. (1). Once this quantity is determined, the quasiclassical CRPs are calculated from it through the use of Eqs. (2) and (3).

To determine the energy dependence of the CRP, the total energy is sampled randomly and uniformly within a preselected $[E_1, E_2]$ interval such that the total energy threshold will be $E_0 \geq E_1$. Once the energy has been selected, the total number of energetically open states of the diatom $n(E)$ is determined, and the initial rovibrational (v, j) state is ran-

domly selected from that set of accessible states. In the next stage, the helicity quantum number is also randomly selected in the above-mentioned interval leading to the initial conditions for each trajectory (the details of the sampling procedure are described in Appendix A of Ref. 52).

When the energy is continuously scanned, $C_r^J(E)$ can be written in terms of a series of Legendre polynomials^{51,59} as

$$C_r^J(E) = \frac{2Q}{E_2 - E_1} \sum_{m=0}^M a_m P_m[x(E)], \quad (5)$$

where $P_m(x)$ is the m th degree Legendre polynomial whose argument is the reduced variable $x(E)$ defined in $[-1, 1]$,

$$x(E) = \frac{2E - E_2 - E_1}{E_2 - E_1}. \quad (6)$$

The normalization constant Q in Eq. (5) is given by

$$Q = \frac{S_r}{N(J)}(E_2 - E_1), \quad (7)$$

where $N(J)$ is the total number of trajectories run in the interval $[E_1, E_2]$ and S_r is the sum of the weights w_i of each individual reactive trajectory, i.e.,

$$S_r = \sum_{i=1}^{N_r} w_i, \quad (8)$$

$$w_i = [2 \min(J_i, j_i) + 1]n(E_i), \quad (9)$$

where E_i , J_i , and j_i are the total energy and the total and rotational angular momentum quantum numbers, respectively, for the i th reactive trajectory, and $n(E_i)$ is the total number of energetically accessible states at E_i .

The QCT calculations were done by running batches of 1.5×10^6 trajectories for selected J values and with total energy values in the 0.27–0.80, 0.23–0.80, and 0.19–0.80 eV ranges for the F+H₂, F+HD, and F+D₂ reactions, respectively. Each individual trajectory was integrated between initial and final points at which the distance between the atom and the center of mass of the diatomic was 8 Å; the integration time step (0.05 fs) was such that energy conservation was better than 1 in 10^5 . The initial rovibrational energies were calculated semiclassically by using the asymptotic diatomic potential energy of the PES; they agree with their exact quantum counterparts within four significant figures.

III. RESULTS AND DISCUSSION

Quasiclassical and QM $C_r^{J=1}(E)$ summed over all the product arrangement channels for the reactions of fluorine atoms with H₂, HD (summing the DF and HF channels), and D₂ molecules are compared in Fig. 1. For the three cases considered, the CRP rises from a threshold and grows in a nearly monotonic way with a smooth step structure superimposed. Since the rovibrational energy levels of the diatoms are more closely spaced following the sequence D₂, HD, and H₂, the magnitude of the CRP at a given total energy is larger for D₂ as compared to HD and H₂. Similarly, the threshold energy E_0 decreases in the sequence H₂, HD, and D₂. The value of E_0 for each of the three isotopomers corresponds

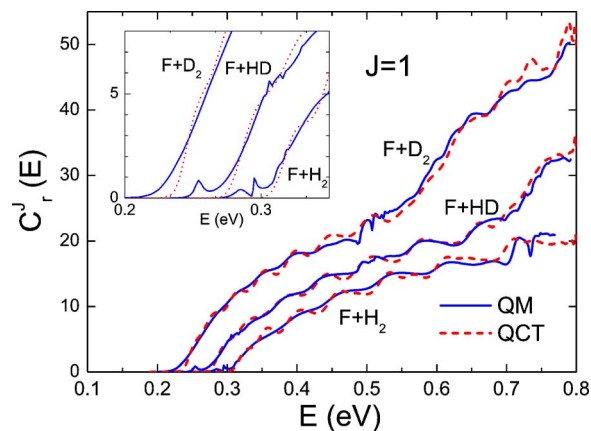


FIG. 1. (Color online) Quantum (solid line) and quasiclassical (dashed line) CRPs for the F+D₂, F+HD, and F+H₂ reactions summed over all product arrangements at $J=1$.

approximately to that of the opening in the $v=0, j=0$ state for each molecule. The ground state energy of the three molecules is larger than that of the barrier in the SW-PES (66.2 meV), and from a purely energetic point of view, the reaction should have no threshold. However, as mentioned above, the early TS closely resembles the isolated molecule in the asymptotic limit, the zero point energy of the TS is only slightly higher than the zero point energy of the reagents, and, consequently, a small amount of translational energy is necessary to surmount the potential barrier. This small translational threshold is very similar to the three isotopic variants,^{15,16} as shown in Fig. 1. The relative magnitude of the CRP at a given energy depends on the number of states available for reaction. A steeper rise in the CRP is observed beyond $E \approx 0.5$ eV for F+D₂ and beyond $E \approx 0.7$ eV for F+HD. This feature is associated with the opening of the $v=1$ reactive channel and will be commented on in more detail below.

A remarkable global similitude between the QM and QCT results is immediately apparent. However, a closer inspection reveals some differences between the two sets of calculations. The quantal $C_r^{J=1}(E)$ extends somewhat below the classical threshold (see inset) due to tunneling and, at some energies, shows sharp peaks or dips most likely associated with resonances.⁶⁰ Note that for F+H₂ and F+HD, there are QM peaks below the classical E_0 . These low-energy QM structures were identified and discussed by Castillo *et al.*¹⁷ In that work, the lowest energy maximum, which is associated with the forward peaks observed in the experiments of Lee and co-workers,⁴ was not attributed to resonances but to tunneling through the combined centrifugal and potential energy barriers. The rest of the peaks in the threshold region were assigned to Feshbach resonances. As far as we know, the higher energy quantal oscillatory structures have not been analyzed in detail.

The wealth of stereodynamic information contained in the helicity dependence of the CRP was emphasized in our recent investigation of the D+H₂ reaction.⁵² In the following paragraphs, k -resolved CRPs are analyzed for F+H₂.

Figure 2 shows the QM $C_r^{J=1,k}(E)$ for the three isotopic variants considered resolved in the helicity quantum numbers

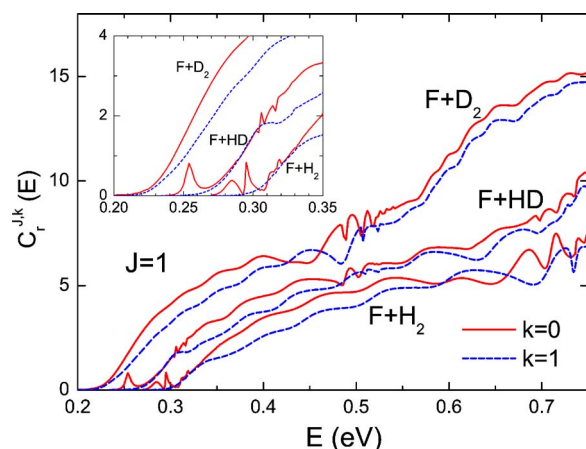


FIG. 2. (Color online) QM CRP resolved in helicity quantum number k for the $F+D_2$, $F+HD$, and $F+H_2$ reactions summed over all product arrangements at $J=1$. $C_r^{J=1,k=0}(E)$, solid line. $C_r^{J=1,k=1}(E)$, dashed line.

$k=0$ and 1. In this representation, some interesting details are disclosed. The CRPs corresponding to $k=0$ are similar in magnitude (only slightly larger) than those for $k=1$ over most of the energy range considered, and a series of k -dependent fast oscillations appear at $E \approx 0.5$ and 0.7 eV. These oscillations cancel out partly in the k -unresolved CRP and leave only the unpronounced narrow features visible in Fig. 1. The low-energy resonances appearing below the classical thresholds (see Fig. 1) for the $F+HD$ and $F+H_2$ reactions are found to correspond to $k=0$. For $k=1$, the resonance structures are absent, and the thresholds are slightly higher for these two reactions. In any case, leaving aside the just mentioned resonances, the $C_r^{J=1,k=0}(E)$ and $C_r^{J=1,k=1}(E)$ have similar thresholds. This result is in contrast to the behavior found in $D+H_2$ (see Fig. 4 of Ref. 52), where a clear upward shift in the CRP threshold was observed with growing k and indicates that a wider range of relative orientations between the rotating molecule and the collision axis is allowed for $F+H_2$.

In Fig. 3, classical and QM $C_r^{J=1,k=0}(E)$ calculations for the two exit channels of the $F+HD$ reaction are compared. In earlier works, valuable information about the dynamics of the reactive system under study could be derived from the asymmetry of this isotopic variant.^{14,16,24,25} Some channel-specific features are observed in the quantal calculations. In the $HF+D$ exit channel, the QM sharp resonance peak below the classical threshold associated with the QM resonance observed in the integral reaction cross section^{24,25} is clearly visible. This channel has also some fast oscillations close to 0.7 eV. The CRP for the $DF+H$ exit channel has less structure but shows also fast oscillations at $E=0.5$ eV. Except for these narrow features the CRPs for the two channels are similar. The global agreement between QM and QCT results is again good, but, as expected, the classical result does not show the fast oscillations or the low-energy peak in the $FH+D$ exit channel. The more classical character of the $DF+H$ channel in the post-threshold region reflected in Fig. 3 was also demonstrated by the successful simulation of the measurements of Lee and co-workers with QCT data.¹⁴ The QCT CRP for the production of HF is somewhat lower than the QM one over the 0.3 – 0.5 eV range, but this difference is

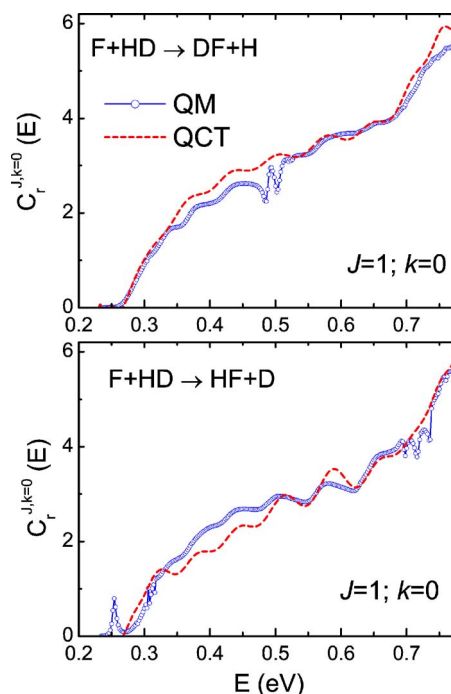


FIG. 3. (Color online) Comparison of QM (open circles, solid line) and QCT (dashed line) $J=1$, $k=0$ CRPs for the $DF+H$ (top) and $HF+D$ (bottom) channels of the $F+HD$ reaction.

compensated in the $DF+H$ channel where the QCT CRP is slightly larger. Over this energy interval, a strong and opposing influence of rotation on the cross section for the production of HF and DF was found in former QCT calculations.¹⁶ For $k=1$, the QM and QCT CRPs for the two channels are shown in Fig. 4. In general terms, they display less structure and the resonances close to the threshold, just mentioned for $k=0$, do not show up here. The agreement between QM and QCT is even better as observed also in the case of the $D+H_2$ reaction.⁵²

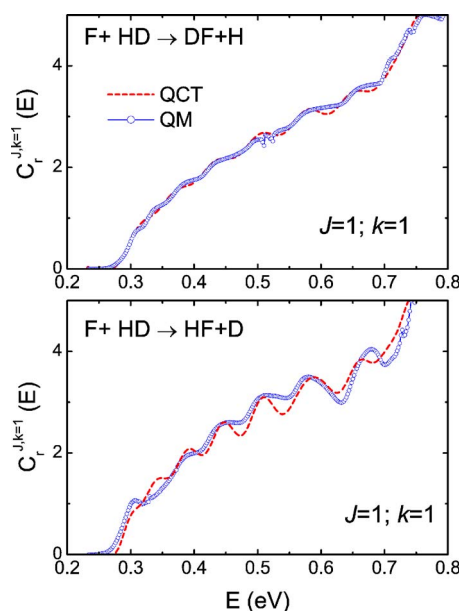


FIG. 4. (Color online) Comparison of QM (open circles, solid line) and QCT (dashed line) $J=1$, $k=1$ CRPs for the $DF+H$ (top) and $HF+D$ (bottom) channels of the $F+HD$ reaction.

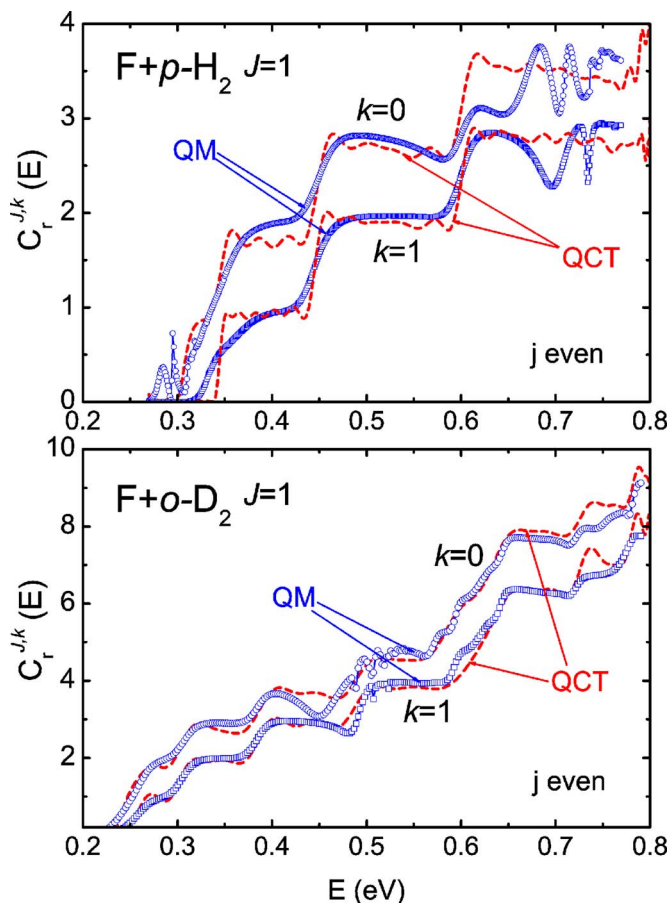


FIG. 5. (Color online) Comparison of QM (open symbols, solid line) and QCT (dashed line) $J=1$ helicity-resolved CRPs for the F + p -H₂ (top) and F + o -D₂ (bottom) (j even) reactions.

In order to analyze the structures appearing in the CRP and their possible association with successive internal states of the reagents, it is pertinent to resolve the CRP into the ortho and para subsets of H₂ and D₂, which are characterized by a wider spacing (two quanta) between successive degrees of rotational excitation. The effect of this wider spacing on the corresponding CRP is shown in Fig. 5 where classical and quantal $C_r^{J=1,k=0,1}(E)$ are shown for the reaction of fluorine atoms with p -H₂ and o -D₂. In the upper panel of Fig. 5, corresponding to F + p -H₂, pronounced steps associated with $\Delta j=2$ increments in the rotational excitation of p -H₂ are seen both for $k=0$ and $k=1$. In the two cases, the QM CRPs are smoother and retain the resonance structures commented on in the previous paragraphs. It is worth noticing that each step has approximately a height of one unit regardless the value of k , thus indicating a transmission coefficient of almost unity.⁴³ The rise in one-unit steps is also apparent in the k -resolved CRP for higher J , as can be seen in QM results portrayed in Fig. 3 of Ref. 20 for $J=6$. The explanation of this fact will be given in the next paragraphs. The smaller spacing between the rotational levels of D₂ is reflected in the less pronounced steps observed in the CRP of F + o -D₂ (lower panel of Fig. 5). Between $E \approx 0.55$ and 0.65 eV, a larger rise in the CRP due to the opening of the first vibrational level of D₂ is observed among the smaller rotational steps. As commented above, the smaller zero-point energy of

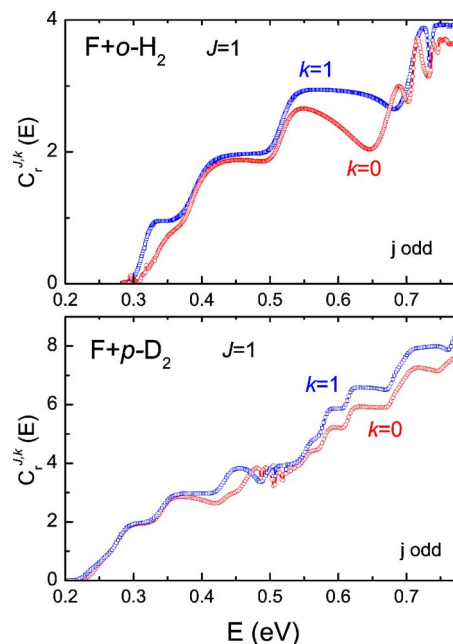


FIG. 6. (Color online) Comparison of QM $J=1$, $k=0$ and $J=1$, $k=1$ helicity-resolved CRPs for the F + o -H₂ (top) and F + p -D₂ (bottom) (j odd) reactions.

the D₂ molecule is responsible for the lower total energy threshold of this reaction. For this heavier isotopic variant, the resonance structures are practically absent since tunneling is much less effective.¹⁷ This is further corroborated by the good agreement between the QM and QCT thresholds for this isotopic variant. Except for the resonance peaks, the good agreement between the QM and QCT results is also maintained at this level of resolution. The first inspection in Fig. 5 suggests the dependence of the CRPs on k , but, in fact, these results reflect only the dependence of the CRP on the j level of the molecular reagents, as discussed in more detail below.

The CRPs obtained for the reaction of fluorine atoms with molecules in odd rotational levels (o -H₂ and p -D₂) are shown in Fig. 6. In contrast to the results of the D + H₂ and other isotopic variants of the H₃ system for which the ortho and para CRPs are almost identical up to $E=1.6$ eV,^{51,61} (although differences are appreciable at higher energies⁵¹), the CRPs of the F + H₂ and F + D₂ for the two nuclear spin species are notably different.

While the CRPs for even rotational levels of $k=0$ and 1 are neatly separated, the curves in Fig. 6 corresponding to odd rotational levels are much closer to each other and even cross at some energies. The QCT CRPs (not shown for clarity) are also in good agreement with the QM results. The reason for the different behaviors observed in Figs. 5 and 6 has to do with the helicity quantum numbers that can be associated with a given j . For p -H₂ and o -D₂, $j=0$ is the first rotational state, and for this state, the only helicity quantum number possible is $k=0$. The helicity quantum number $k=1$ is first encountered in $j=2$ and, consequently, the CRP of $k=1$ will have a larger threshold. The energy difference between the two thresholds corresponds roughly to that of the energy levels $j=0$ and $j=2$ of the molecules, which strongly

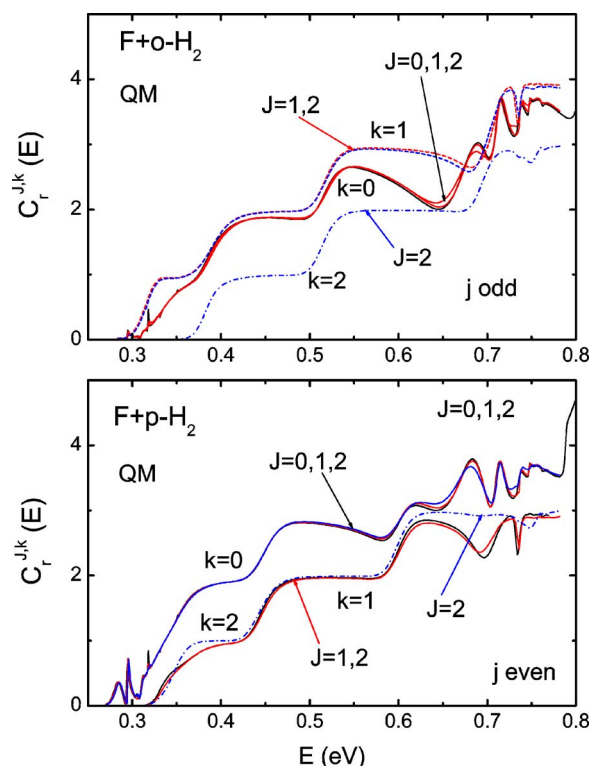


FIG. 7. (Color online) QM helicity-resolved ($k=0, 1, 2$) CRP for $J=0, 1, 2$. Top: $F+o\text{-H}_2$ (j odd). Bottom: $F+p\text{-H}_2$ (j even). The various $C_r^{J,k}(E)$ for different J values at the same k are almost indistinguishable.

suggests that the threshold shift observed in Fig. 5 reflects an energy dependence (the opening of the successive j states) rather than a k dependence. For $o\text{-H}_2$ and $p\text{-D}_2$, both $k=0$ and $k=1$ contribute to the CRP of the first rotational level, which is now $j=1$. In this case, the two k -resolved CRPs have the same threshold and a more parallel growth.

In order to clarify this point further, we have represented in Fig. 7 the $C_r^{J,k}(E)$ of the $F+o\text{-H}_2$ and the $F+p\text{-H}_2$ reactions for $J=0-2$ and $k=0-2$. In the reaction with $o\text{-H}_2$ (upper panel), the first rotational level is $j=1$. For this level, k can take the absolute values of 0 and 1. The upper panel of the figure shows that the threshold and post-threshold rises for the two k values are relatively similar. The reaction for helicity number $k=2$ only takes place above the threshold for $j=3$, which is the next rotational level of $o\text{-H}_2$. In the case of $p\text{-H}_2$, the first rotational level is $j=0$ for which only $k=0$ is allowed (see lower panel of Fig. 7), and consequently the $C_r^{J,k=0}(E)$ has the lowest threshold. For $j=2$, which is next in the $p\text{-H}_2$ level series, rotational levels $j=2$, $k=1$, and $k=2$ are also possible, and the CRPs for these two helicity values open simultaneously when the $j=2$ threshold is reached. After the threshold, the two $C_r^{J,k}(E)$ have very similar shapes.

Note that for a given k , the results corresponding to the various values of the total angular momentum J are practically indistinguishable, a fact that is also observed for the $D+\text{H}_2$ reaction.⁵² Only at sufficiently high J values, the effect of the centrifugal barrier will cause an upward shift in the threshold. The appearance of CRPs with similar thresholds and shapes for different k numbers displayed in Figs. 6

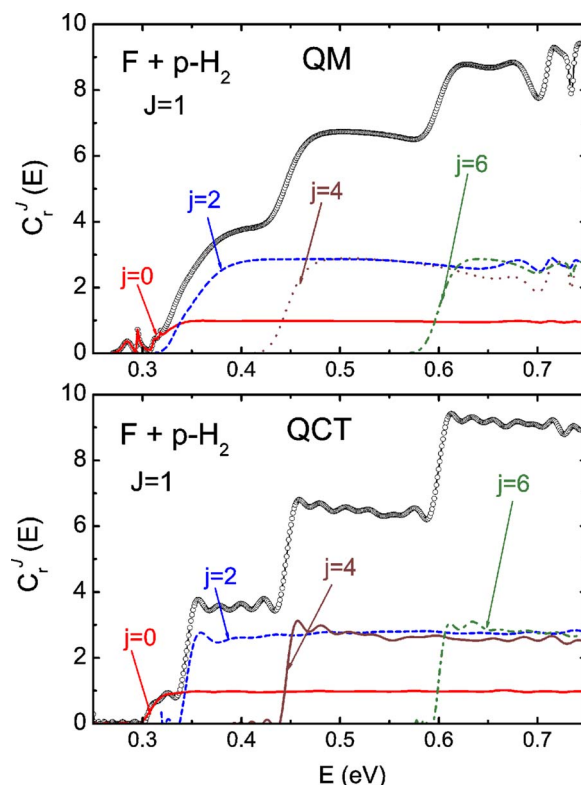


FIG. 8. (Color online) Decomposition of the $F+p\text{-H}_2$, $J=1$ CRP (summed over the $k=0, \pm 1$ helicity components) in terms of the contributions from various (even) rotational levels ($j=0-6$). Top: QM results. Bottom: QCT results.

and 7 is in marked contrast to the behavior observed in our previous work on $D+\text{H}_2$,⁵² where a clear k specificity in the CRP threshold was observed in all cases.

Further insight into the characteristics of the TS can be gained from the consideration of the rotationally state-resolved CRP. The contribution of the different internal states of hydrogen and deuterium to the CRP is shown in detail in Figs. 8 and 9. In these figures, the QM and QCT total CRP and the j resolved CRPs (summed over k), are represented for the $F+p\text{-H}_2$ and $F+o\text{-D}_2$ reactions, respectively. The various v and j contributions to the CRP have a similar structure; they increase steeply from their corresponding thresholds, which correspond roughly with the opening of the successive rotational (rovibrational) states, and then get stabilized and form a plateau with a constant value common for all $j>0$ over the energy range considered. For $j=0$, the height of the plateau is about one third of that for $j>0$. The QCT steps are more pronounced, rising quickly from their respective thresholds, which are systematically higher than those from the QM calculations (by about 40 meV). This difference can be obviously traced back to the absence of tunneling in the QCT data. In spite of this difference, there is a very good agreement between the QM and QCT results in the rotationally state-resolved CRPs. In the QM results for $F+\text{H}_2$, the oscillatory structures at 0.7 and 0.75 eV appear with varying intensities but at the same energy for the different j -resolved CRPs. These features add constructively in the j -summed CRP where they become more pronounced (see upper panel of Fig. 8).

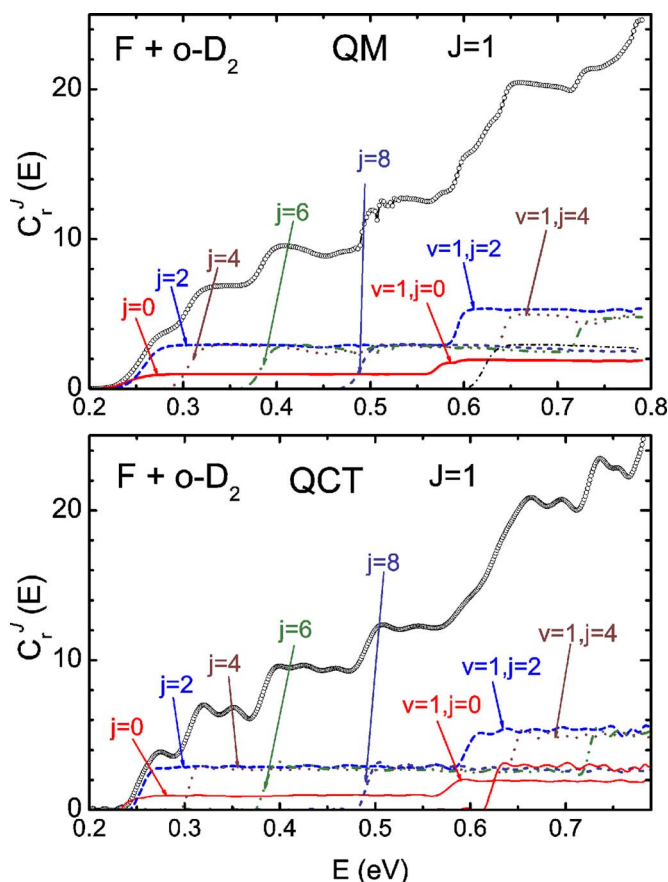


FIG. 9. (Color online) Decomposition of the F+*o*-D₂, *J*=1 CRP (summed over the *k*=0, ±1 components) in terms of the contributions from various (even) rovibrational levels (*v*=0, *j*=0–8, *v*=1, *j*=0–6). Top: QM results. Bottom: QCT results.

The smaller CRP value for *j*=0 is due to the existence of only one helicity projection for this value of *j*. For *j*>0, *k*=1 and *k*=−1 participate also in the reaction and increase the value of the CRP for *J*=1. The results of Figs. 8 and 9 also indicate that in the plateau region, each of the three possible *k* values contributes roughly equally to the CRP for a given *j*. It can thus be concluded that the reaction is relatively insensitive to the orientation of the H₂ or D₂ molecules.

For F+*o*-D₂ in Fig. 9, the opening of the first vibrational state takes place at about 0.57 eV. Between this value and 0.67 eV, the levels *v*=1, *j*=0; *v*=1, *j*=2; *v*=0, *j*=10; and *v*=1, *j*=4 become open and cause the marked increase observed in the total CRP over this energy range.

The results just shown clearly demonstrate that each step of the CRPs is due to the opening of the successive rovibrational states of the H₂ and D₂ molecules, which, given the quasiadiabatic character of the internal motion,⁵³ corresponds also to the opening of the successive TS levels.⁴³ Their respective thresholds nearly coincide with the total energy that is necessary to bring forth a given rovibrational state. More importantly, the height of each step basically reflects the number of *k* values consistent with each *j* and *J*, thus indicating that the thresholds for the appearance of the various *k* states are practically the same and each *k* contributes to the total CRP with the same weight.

The pronounced step structure found in the CRPs of the reactions of F with *o*-H₂ and *p*-H₂ is in strong contrast to the rather smooth evolution obtained previously for the H+H₂ system⁵¹ and its isotopomers (see, for instance, Fig. 9 of Ref. 51). The resolution of the CRP into the rotational states of the reagents helps illustrate the properties of the TS and the reasons of the different reactivities of the H+H₂ and F+H₂ systems.

The F+H₂ reaction is essentially barrierless; the potential barrier is very low and poses only a small hindrance to reaction, which is easily overcome with a small amount of translational energy. Once this barrier is surmounted, the evolution of various CRPs with energy reflects gradual contribution of successive internal states of H₂ to the reaction. The fact that the CRPs are nearly independent of *k* (see discussions of Figs. 5–8 and the results shown in Fig. 3 of Ref. 20) shows that there are hardly any steric restrictions in the course of reactive collisions at least for values of *J* up to *J*=6. This fact is also reflected in the sharpness of the steps in the *j*-resolved CRPs, which indicates that for a given *j*, all possible orientations of the plane of rotation with respect to the collision vector (*k* values) open at the same time. Note again that these steps reflect the quantization in the entrance channel, which, in this case, is almost coincident with that in the early TS.⁴³

In the H+H₂ reaction, the barrier height corresponds to a total energy of approximately 0.6 eV. At this energy, a significant number of rotational states of the molecules (up to *j*=6) can be populated. The threshold and the smooth post-threshold rise in the CRP are not determined by the gradual opening of the various rotational channels of H₂, but by the steric restrictions imposed by the potential that are manifested in the slower rise of the CRP with energy and clear helicity quantum number dependence observed in the CRPs in the H₃ system.^{51,52} The barrier for this reaction has a strong dependence on the attacking angle increasing rapidly as the three-atom system departs from collinearity. In consequence, not all orientations (*k* values) become open when the threshold of a given *j* is reached, and this is clearly reflected in the CRP.

IV. SUMMARY AND CONCLUSIONS

Throughout this work, it has been shown that the combination of QM and QCT calculations of specific CRPs provides a powerful tool for the systematization of reaction types in terms of TS properties, the identification of pure QM effects, and the interpretation of stereodynamical characteristics. The advantages of this combined quasiclassical and QM approaches, which was first tried on the prototypical H+H₂ system in a previous work, are demonstrated here through the application of the method to a reaction with markedly different dynamical characteristics. Specifically, a QM and quasiclassical comparative study of the CRPs of the F+H₂, D₂, and HD has been presented for total angular momenta *J*=0–2. The QCT method is based on the quantization not only of the initial reagent states but also of the total angular momentum and its projection along the relative velocity vector, i.e., the helicity. The main goal of this work is

to extract some information about the energetic structure of the TS and the stereodynamics of these reactions and compare the results to those found for the H_3 reactive system.

In general terms, a very good agreement is found between the exact QM and QCT CRPs at all levels of resolution, with the exception of somewhat smaller total energy thresholds and the resonance structures observed in the QM results at low collision energies for the $F+H_2$ and the $HF+D$ channels of the $F+HD$ reaction. In addition, some fast oscillations are found in the QM results in the CRP at around 0.5 and 0.7 eV total energies, which do not have correspondence in the QCT case.

The QM and QCT CRPs have been analyzed in terms of the resolved contributions from the different helicity quantum numbers k . It has been found that the k -resolved CRPs are similar when summed over all rotational states. This is in contrast to the results for the $D+H_2$ reaction where the thresholds and magnitudes of the k -resolved CRPs change strongly with increasing k . More interesting is the analysis in ortho and para species for the $F+H_2$ and $F+D_2$ reactions. A pronounced steplike structure is found in both cases, which is even more conspicuous in the QCT results. The apparent differences in the thresholds and magnitudes between the k -resolved CRPs for even and odd rotational states can be traced back to the participation of the various rovibrational states compatible with a given k value. Indeed, the decomposition of the CRP in the contributions of various j states clearly demonstrates that each step is due to the opening of successive rovibrational states of the H_2 and D_2 molecules, which for this reaction coincides practically with the energy levels of the early TS. Their respective thresholds nearly coincide with the total energy necessary to open a given rovibrational state. In addition, the height of each step basically reflects the number of k values consistent with each j and J , thus indicating that all possible k states come forth simultaneously contributing with the same weight of almost unity. The main conclusion is that no steric restrictions exist at least at relatively low J values, and all orientations have similar reactivity. This finding is not surprising since the TS is loose with a wide cone of acceptance for the reaction.

The comparison of the $F+H_2$ reaction with $D+H_2$ is illustrative. In both cases, for a given k value, the CRPs are practically independent of the total angular momentum for low J (as long as the centrifugal barrier does not come into play). However, for the latter reaction, a strong dependence with k was found in the k -resolved CRP with increasing thresholds and decreasing magnitudes as k increases, indicating substantial steric constraints due to its strongly collinearly dominated TS. In contrast, for the title reaction, apart from the effects at low energies, which only appear for $k=0$, the magnitude and the thresholds of the k resolved CRPs are very similar.

This study shows that the CRP, in spite of being a strongly averaged magnitude, is extremely useful to unveil the stereodynamics of a reaction especially when it is analyzed in terms of the contribution of the helicity quantum numbers.

ACKNOWLEDGMENTS

This work was financed by the Spanish Ministry of Education and Science (Grant Nos. CTQ2005-08493, ENE2006-14577-C04-C03/FTN, and FIS2007-61686). The research was performed within the Unidad Asociada “Química Física Molecular” between the Universidad Complutense and the CSIC.

- ¹M. J. Berry, *J. Chem. Phys.* **59**, 6229 (1973), and references therein.
- ²D. S. Perry and J. C. Polanyi, *Chem. Phys.* **12**, 419 (1976), and references therein.
- ³D. M. Neumark, A. M. Wodtke, G. N. Robinson, C. C. Hayden, R. Shobatake, R. K. Sparks, T. P. Schafer, and Y. T. Lee, *J. Chem. Phys.* **82**, 3045 (1985).
- ⁴D. M. Neumark, A. M. Wodtke, G. N. Robinson, C. C. Hayden, and Y. T. Lee, *J. Chem. Phys.* **82**, 3067 (1985).
- ⁵M. Faubel, L. Rusin, S. Schlemmer, F. Sundermann, U. Tappe, and J. P. Toennies, *J. Chem. Phys.* **101**, 2106 (1994).
- ⁶M. Faubel, B. Martínez-Haya, L. Y. Rusin, U. Tappe, and J. P. Toennies, *Chem. Phys. Lett.* **232**, 197 (1995).
- ⁷M. Faubel, B. Martínez-Haya, L. Y. Rusin, U. Tappe, and J. P. Toennies, *Z. Phys. Chem.* **188**, 197 (1995).
- ⁸A. Weaver and D. M. Neumark, *Faraday Discuss. Chem. Soc.* **91**, 5 (1991).
- ⁹S. E. Bradforth, D. W. Arnold, D. M. Neumark, and D. E. Manolopoulos, *J. Chem. Phys.* **99**, 6345 (1993).
- ¹⁰D. E. Manolopoulos, K. Stark, H.-J. Werner, D. W. Arnold, S. E. Bradforth, and D. M. Neumark, *Science* **262**, 1852 (1993).
- ¹¹K. Stark and H.-J. Werner, *J. Chem. Phys.* **104**, 6515 (1996).
- ¹²F. J. Aoiz, L. Bañares, V. J. Herrero, V. Sáez Rábanos, K. Stark, and H.-J. Werner, *Chem. Phys. Lett.* **223**, 215 (1994).
- ¹³F. J. Aoiz, L. Bañares, V. J. Herrero, V. Sáez Rábanos, K. Stark, and H.-J. Werner, *J. Phys. Chem.* **98**, 10665 (1994).
- ¹⁴F. J. Aoiz, L. Bañares, V. J. Herrero, V. Sáez Rábanos, K. Stark, and H.-J. Werner, *J. Chem. Phys.* **102**, 9248 (1995).
- ¹⁵F. J. Aoiz, L. Bañares, V. J. Herrero, K. Stark, and H.-J. Werner, *Chem. Phys. Lett.* **254**, 341 (1996).
- ¹⁶F. J. Aoiz, L. Bañares, V. J. Herrero, V. Sáez Rábanos, K. Stark, I. Tanarro, and H.-J. Werner, *Chem. Phys. Lett.* **262**, 175 (1996).
- ¹⁷J. F. Castillo, D. W. Manolopoulos, K. Stark, and H.-J. Werner, *J. Chem. Phys.* **104**, 6531 (1996).
- ¹⁸F. J. Aoiz, L. Bañares, B. Martínez-Haya, J. F. Castillo, K. Stark, and H.-J. Werner, *J. Phys. Chem. A* **101**, 6403 (1997).
- ¹⁹J. F. Castillo, B. Hartke, H.-J. Werner, F. J. Aoiz, L. Bañares, and B. Martínez-Haya, *J. Chem. Phys.* **109**, 7224 (1998).
- ²⁰F. J. Aoiz, L. Bañares, and J. F. Castillo, *J. Chem. Phys.* **111**, 4013 (1999).
- ²¹W. B. Chapman, B. W. Blackmon, and D. J. Nesbitt, *J. Chem. Phys.* **107**, 8193 (1997).
- ²²W. W. Harper, S. A. Nizkorodov, and D. J. Nesbitt, *J. Chem. Phys.* **116**, 5622 (2002).
- ²³M. H. Alexander, D. E. Manolopoulos, and H.-J. Werner, *J. Chem. Phys.* **113**, 11084 (2000).
- ²⁴R. Skodje, D. Skouteris, D. E. Manolopoulos, S.-H. Lee, F. Dong, and K. Liu, *J. Chem. Phys.* **112**, 4536 (2000).
- ²⁵R. Skodje, D. Skouteris, D. E. Manolopoulos, S.-H. Lee, F. Dong, and K. Liu, *Phys. Rev. Lett.* **85**, 1206 (2000).
- ²⁶Y. Zhang, T. X. Xie, K. L. Han, and J. Z. H. Zhang, *J. Chem. Phys.* **119**, 12921 (2003).
- ²⁷V. Aquilanti, S. Cavali, A. Simoni, A. Aguilar, J. M. Lucas, and D. De Fazio, *J. Chem. Phys.* **121**, 11675 (2004).
- ²⁸V. Aquilanti, S. Cavali, D. De Fazio, A. Simoni, and T. V. Tscherebul, *J. Chem. Phys.* **123**, 054314 (2005).
- ²⁹M. Hayes, M. Gustafson, A. M. Mebel, and R. T. Skodje, *Chem. Phys.* **308**, 259 (2005).
- ³⁰M. Qiu, Z. Ren, L. Che, D. Dai, S. A. Harich, X. Wang, X. Yang, C. Xu, D. Xie, M. Gustafson, R. T. Skodje, Z. Sun, and D. H. Zhang, *Science* **311**, 1440 (2006).
- ³¹Z. Ren, L. Che, M. Qui, X. Wang, D. Dai, S. A. Harich, X. Wang, X. Yang, C. Xu, D. Xie, Z. Sun, and D. H. Zhang, *J. Chem. Phys.* **125**, 151102 (2006).
- ³²L. Che, Z. Ren, X. Wang, W. Dong, D. Dai, X. Wang, D. H. Zhang, X.

- Yang, L. Sheng, G. Li, H.-J. Werner, F. Lique, and M. H. Alexander, *Science* **317**, 1061 (2007).
- ³³ F. Lique, M. H. Alexander, G. Li, H.-J. Werner, S. A. Nizkorodov, W. W. Harper, and D. J. Nesbitt, *J. Chem. Phys.* **128**, 084313 (2008).
- ³⁴ W. H. Miller, *J. Chem. Phys.* **61**, 1823 (1974).
- ³⁵ W. H. Miller, *J. Chem. Phys.* **62**, 1899 (1975).
- ³⁶ S. Chapman, S. M. Hornstein, and W. H. Miller, *J. Am. Chem. Soc.* **97**, 892 (1975).
- ³⁷ W. H. Miller, *J. Chem. Phys.* **65**, 2216 (1976).
- ³⁸ W. H. Miller, *Acc. Chem. Res.* **9**, 306 (1976).
- ³⁹ W. H. Miller, *Acc. Chem. Res.* **26**, 174 (1993).
- ⁴⁰ D. C. Chatfield, R. S. Friedman, D. G. Truhlar, B. C. Garrett, and D. W. Schwenke, *J. Am. Chem. Soc.* **113**, 486 (1991).
- ⁴¹ D. C. Chatfield, R. S. Friedman, D. G. Truhlar, and D. W. Schwenke, *Faraday Discuss. Chem. Soc.* **91**, 289 (1991).
- ⁴² D. C. Chatfield, R. S. Friedman, D. W. Schwenke, and D. G. Truhlar, *J. Phys. Chem.* **96**, 2414 (1992).
- ⁴³ D. C. Chatfield, R. S. Friedman, S. L. Mielke, G. C. Lynch, T. C. Allison, D. G. Truhlar, and D. W. Schwenke, in *Dynamics of Molecules and Chemical Reactions*, edited by R. E. Wyatt and J. Z. H. Zhang (Dekker, New York, 1996).
- ⁴⁴ D. C. Chatfield, S. L. Mielke, T. C. Allison, and D. G. Truhlar, *J. Chem. Phys.* **112**, 8387 (2000).
- ⁴⁵ D. Dai, C. C. Wang, S. A. Harich, X. Wang, X. Yang, S. D. Chao, and R. Skodje, *Science* **300**, 1730 (2003).
- ⁴⁶ R. T. Skodje and X. Yang, *Int. Rev. Phys. Chem.* **23**, 253 (2004).
- ⁴⁷ M. Gustafsson and R. T. Skodje, *J. Chem. Phys.* **124**, 144311 (2006).
- ⁴⁸ J. Zhang, D. Dai, C. C. Wang, S. A. Harich, X. Wang, X. Yang, M. Gustafsson, and R. T. Skodje, *Phys. Rev. Lett.* **96**, 093201 (2006).
- ⁴⁹ M. Gustafsson, R. T. Skodje, J. Zhang, D. Dai, S. A. Harich, X. Wang, and X. Yang, *J. Chem. Phys.* **124**, 241105 (2006).
- ⁵⁰ M. Gustafsson and R. T. Skodje, *Chem. Phys. Lett.* **434**, 20 (2007).
- ⁵¹ F. J. Aoiz, M. Brouard, C. Eyles, J. F. Castillo, and V. Sáez Rábanos, *J. Chem. Phys.* **125**, 144105 (2006).
- ⁵² F. J. Aoiz, V. J. Herrero, M. P. de Miranda, and V. Sáez Rábanos, *Phys. Chem. Chem. Phys.* **9**, 5367 (2007).
- ⁵³ S.-F. Wu and R. A. Marcus, *J. Chem. Phys.* **56**, 3519 (1972), and references therein.
- ⁵⁴ D. W. Schwenke, R. Steckler, F. B. Brown, and D. G. Truhlar, *J. Chem. Phys.* **84**, 5706 (1986).
- ⁵⁵ S. L. Mielke, G. C. Lynch, D. G. Truhlar, and D. W. Schwenke, *Chem. Phys. Lett.* **213**, 10 (1993).
- ⁵⁶ F. J. Aoiz, L. Bañares, V. J. Herrero, and V. Sáez Rábanos, *Chem. Phys.* **187**, 227 (1994).
- ⁵⁷ F. J. Aoiz, V. Sáez Rábanos, B. Martínez-Haya, and T. González-Lezana, *J. Chem. Phys.* **123**, 094101 (2005).
- ⁵⁸ D. Skouteris, J. F. Castillo, and D. E. Manolopoulos, *Comput. Phys. Commun.* **133**, 128 (2000).
- ⁵⁹ N. C. Blais and D. G. Truhlar, *J. Chem. Phys.* **67**, 1540 (1977).
- ⁶⁰ G. C. Lynch, P. Halvick, M. Zhao, D. G. Truhlar, C. Yu, D. J. Kouri, and D. W. Schwenke, *J. Chem. Phys.* **94**, 7150 (1991).
- ⁶¹ S. L. Mielke, G. C. Lynch, D. G. Truhlar, and D. W. Schwenke, *J. Phys. Chem.* **98**, 8000 (1994).